GATE V6: a major enhancement of the GATE simulation platform enabling modelling of CT and radiotherapy

2011 Phys. Med. Biol. 56 881

(http://iopscience.iop.org/0031-9155/56/4/001)

Phys. Med. Biol. **56** (2011) 881–901 doi:10.1088/0031-9155/56/4/001

GATE V6: a major enhancement of the GATE simulation platform enabling modelling of CT and radiotherapy

S Jan[1], D Benoit[2], E Becheva[1], T Carlier[3,4], F Cassol[5], P Descourt[6], T Frisson[7], L Grevillot[7], L Guigues[7], L Maigne[8], C Morel[5], Y Perrot[8], N Rehfeld[2], D Sarrut[7], D R Schaart[9], S Stute[2], U Pietrzyk[10], D Visvikis[6], N Zahra[7] and I Buvat[2]

[1] DSV/I2BM/SHFJ, Commissariat à l'Energie Atomique, Orsay, France
[2] IMNC–UMR 8165 CNRS–Paris 7 and Paris 11 Universities, 15 rue Georges Clémenceau, 91406 Orsay Cedex, France
[3] INSERM U892–Cancer Research Center, University of Nantes, Nantes, France
[4] Nuclear Medicine Department, University Hospital of Nantes, Nantes, France
[5] Centre de physique des particules de Marseille, CNRS-IN2P3 and Université de la Méditerranée, Aix-Marseille II, 163, avenue de Luminy, 13288 Marseille Cedex 09, France
[6] INSERM, U650, Laboratoire du Traitement de l'Information Medicale (LaTIM), CHU Morvan, Brest, France
[7] Université de Lyon, CREATIS, CNRS UMR5220, Inserm U630, INSA-Lyon, Université Lyon 1, Centre Léon Bérard, France
[8] Laboratoire de Physique Corpusculaire, 24 Avenue des Landais, 63177 Aubière Cedex, France
[9] Delft University of Technology, Radiation Detection & Medical Imaging, Mekelweg 15, 2629 JB Delft, The Netherlands
[10] Reseach Center Juelich, Institute of Neurosciences and Medicine and Department of Physics, University of Wuppertal, Germany

E-mail: buvat@imnc.in2p3.fr

Received 6 August 2010, in final form 29 November 2010
Published 19 January 2011
Online at stacks.iop.org/PMB/56/881

Abstract

GATE (Geant4 Application for Emission Tomography) is a Monte Carlo simulation platform developed by the OpenGATE collaboration since 2001 and first publicly released in 2004. Dedicated to the modelling of planar scintigraphy, single photon emission computed tomography (SPECT) and positron emission tomography (PET) acquisitions, this platform is widely used to assist PET and SPECT research. A recent extension of this platform, released by the OpenGATE collaboration as GATE V6, now also enables modelling of x-ray computed tomography and radiation therapy experiments. This paper presents an overview of the main additions and improvements implemented in GATE since the publication of the initial GATE paper (Jan *et al* 2004 *Phys. Med. Biol.* **49** 4543–61). This includes new models available in GATE to simulate optical and hadronic processes, novelties in modelling tracer, organ or detector motion, new options for speeding up GATE simulations, examples illustrating the use of GATE V6 in radiotherapy applications and

CT simulations, and preliminary results regarding the validation of GATE V6 for radiation therapy applications. Upon completion of extensive validation studies, GATE is expected to become a valuable tool for simulations involving both radiotherapy and imaging.

(Some figures in this article are in colour only in the electronic version)

1. Introduction

GATE (Geant4 Application for Emission Tomography) is a Monte Carlo simulation platform developed by the OpenGATE collaboration since 2001 and first publicly released in 2004. Initially, this platform was dedicated to the modelling of planar scintigraphy, single photon emission computed tomography (SPECT) and positron emission tomography (PET) acquisitions (Santin *et al* 2003, Jan *et al* 2004). Over the years, the features of the platform have been enhanced and new versions of the software have been regularly released, to incorporate well-validated upgrades and to stay consistent with regular GEANT4 public releases. Compared to the functionalities of the platform described in the initial paper of the OpenGATE collaboration (Jan *et al* 2004), the major enhancements consist of additional options for speeding up simulations (Taschereau and Chatziioannou 2008, Rehfeld *et al* 2009, Descourt *et al* 2010), facilities to use GATE for dose calculations in internal dosimetry (Visvikis *et al* 2006a, Taschereau and Chatziioannou 2007, Ferrer *et al* 2007, Thiam *et al* 2008, Grevillot *et al* 2010b), and inclusion of optical physics models for accurate modelling of the detector response (van Der Laan *et al* 2010). All these developments have been incorporated in the new GATE V6 release presented here, but are not described in this paper as they have been explained in the articles listed above. Other developments relating to early GATE versions have been reported (Staelens *et al* 2006, De Beenhouwer *et al* 2007, 2008) but were not included in GATE V6 as they have not yet been made available to the OpenGATE collaboration.

In the same period, GATE has been widely used as a tool to assist SPECT and PET research and developments and a number of conventional SPECT and PET scanners and prototypes have been modelled (e.g., Gonias *et al* 2007, Van Der Laan *et al* 2007, Bruyndonckx *et al* 2007, Karakatsanis *et al* 2006, Lamare *et al* 2006, Schmidtlein *et al* 2006, Visvikis *et al* 2006b, Chung *et al* 2005, Assié *et al* 2005, Jan *et al* 2005). More recently, GATE has also been used to model x-ray computed tomography (CT) scanners (Cassol Brunner *et al* 2009, Nicol *et al* 2009, Chen *et al* 2009).

The GATE V6 version released in February 2010 has been considerably extended to enable modelling of radiation therapy experiments. These developments have been largely motivated by the more and more frequent integration of radiotherapy and imaging. Examples of such integration are the use of PET imaging to delineate the metabolically active tumour to be treated by radiotherapy (Ford *et al* 2009) and the emerging domain of in-beam imaging in proton and ion therapy (Crespo *et al* 2007, Knopf *et al* 2008, Nishio *et al* 2006, Parodi *et al* 2008). These developments create a need for tools that enable simultaneous modelling of imaging and radiotherapy experiments.

In this work we present an overview of the main additions and improvements implemented in GATE since the publication of the initial GATE paper (Jan *et al* 2004). We focus on the functionalities that have not yet been reported upon in the specific papers cited above. In section 2, we briefly describe the main improvements made to GATE's architecture. Section 3 describes the new models available in GATE to simulate optical and hadronic processes. Section 4 presents novelties in modelling tracer, organ and detector motion while section 5

explains how CT scans can be modelled with GATE. In section 6, new options for speeding up GATE simulations are given. Section 7 describes new facilities for handling input and output data. A new benchmark is presented in section 8, and section 9 gives preliminary results regarding the validation of GATE V6 for radiation therapy applications. Additional examples illustrating the use of GATE V6 in radiotherapy applications and CT simulations are provided in section 10 and in a companion paper (Grevillot *et al* 2010b). Section 11 gives an overview of upcoming developments in GATE.

2. New features in the architecture of GATE

The basic architecture of the GATE code remains identical to that described in Jan *et al* (2004). It consists of a Geant4 kernel surrounded by three specific layers: (1) the core layer defining the basic simulation elements such as geometry definition, source definition, physical processes, particle tracking, and time management; (2) the application layer, using the basic elements of the core layer, to model objects and processes specific to the imaging applications and, as of version 6, radiotherapy applications; and (3) the user layer, providing the user with simple mechanisms to set up a simulation using scripts only, without any C++ coding. In GATE V6, major changes have been inserted at the first two levels. No major change has been introduced at the user layer.

2.1. Core layer

The changes introduced in the core layer are meant to facilitate future developments in GATE, by introducing a 'plugin' approach, the so-called *auto-list* mechanism, to manage lists of object types involved in the simulations. An object can, for instance, be a volume or a physics process. As an example, adding a new type of geometrical volume (used to describe part of a phantom or a detector) in GATE now only requires inheriting from a Geant4 base class and putting the new source file in the appropriate directory, while no change in other files is necessary; the new type will be automatically inserted in the list of available types.

The most significant parts of the code benefiting from these changes are the volume management for the definition of the simulation geometry (as in the example given above) and the management of the physics processes—hadronic interactions are now available. Cuts (i.e. criteria specifying when secondary particles should not be produced) can also be controlled in a flexible way. Furthermore, the management of sources is now inherited directly from the Geant4 classes and options are provided to move sources within the simulation scene (see section 4). Last but not least, the initialization mechanisms (cross-section table computation) and the run management (data information related to event collection inside a run) of the code were simplified.

Another important feature introduced into the core layer is the concept of *actor*. An *actor* is similar to a sensitive detector (SD) in Geant4 but has extended capabilities; it can store information at each *step* (similar to an SD), but it can also act on particles at each *step*, *track*, *event* or *run*, where the words *step*, *track*, *event* and *run* have the same meanings as in Geant4. For instance, a *DoseActor* measures the energy deposited in a given volume, the *KillActor* stops the tracking of particles when they reach a given volume, the *SimulationStatisticsActor* gives the number of run, events, track, geometrical and physical steps of the simulation, and the *PhaseSpaceActor* stores information related to incoming particles (see section 7).

The concept of *filter* has furthermore been added to GATE to modify the behaviour of *actors*. *Filters* perform tests on the particle properties (e.g., energy, type, or position) at the *step track*, *event*, or *run* level so as to trigger the *actor* only if the test output is true. For

instance, a *filter* can be used to calculate a dose distribution only for electrons having an energy greater than a certain threshold. *Actors* and *filters* can be combined to get new outputs.

Developers can add new types of *actors* and *filters* easily by using the *auto-list* concept.

2.2. Application layer

Contrary to initial GATE versions in which the application layer only managed imaging applications, the application layer is now organized into three distinct parts.

- The imaging application level includes dedicated input and output management, digitizer modules to model the electronic response of various types of detector and a concept of systems to fit scanners of different modalities such as CT, SPECT and PET.
- The new radiotherapy and dosimetry application level includes a new management of particle interactions and provides a new output format appropriate for dose map computation.
- The new general application level gives the users great flexibility in designing a simulation, in a way close to that offered by Geant4. In this general application level, the user can use GATE using script language only or can modify and extend it via C++ programming.

3. Electromagnetic and hadronic physics

In Geant4, each physics process is described by a model (several models are sometimes available for a given physics process) and a corresponding cross-section table. All Geant4 physics models and cross-sections below 10 GeV are now available in GATE. In particular, models describing the transport of optical photons and hadronic interactions have recently been introduced. New processes can easily be added thanks to the *auto-list* concept.

3.1. Optical and scintillation processes

Optical photons can be considered the primary information carriers in scintillation detectors such as those used in SPECT and PET. However, since a large number of scintillation photons (up to $\sim 10^4$) may be generated per absorbed gamma quantum, it is generally not practical to include optical transport in the simulation of a full SPECT or PET system. Optical simulations can nevertheless be useful, for example at the level of single detectors. Such simulations may help to better understand the performance of existing systems and assist in research on novel detector concepts. GATE has therefore been extended to make it possible to simulate the scintillation process, the transport of scintillation photons through the crystal to the light sensor and the conversion of these photons into electronic signals, using the scintillation and optical transport models available in Geant4.

The Geant4 optical models were originally derived from Detect2000 (Levin and Moisan 1996). For example, they allow for the time- and wavelength-dependent modelling of the scintillation process; absorption and scattering of optical photons within dielectric materials; and reflection, transmission and absorption at various types of material interfaces (dielectric–dielectric, dielectric–metal, etc) with different surface treatment (optically polished, ground, etched).

In general, optical Monte Carlo simulations require knowledge of a relatively large number of input parameters such as the light yield, energy resolution, emission spectrum and decay characteristics of the scintillator; the refractive index, absorption length, scattering length and surface roughness of the crystal, and the reflection and absorption properties of the light sensor

and any other materials surrounding the crystal. Sometimes these parameters can be obtained from published data, and sometimes they need to be determined experimentally.

Van der Laan *et al* (2010) recently published a validation of the GATE optical routines by comparing simulated results with measurements on a prototype monolithic PET detector. That work and the references therein provide more details on the optical models used in GATE. The same work also illustrates how the required optical input parameters can be determined. An example of a GATE script for performing optical simulations is provided with the GATE release. Other examples of GATE optical Monte Carlo simulations have been published (Janecek and Moses 2010, van Der Laan *et al* 2006).

3.2. Electromagnetic processes

In GATE V6, three packages of models/cross-sections are available to simulate electromagnetic processes: the standard package for processes between 1 keV and 100 TeV, the low-energy package for processes between 250 eV and 100 GeV, and the PENELOPE package for processes between 250 eV and 1 GeV. Models and cross-sections are based on theoretical calculations and on experimental data. The standard package relies on the parameterization of experimental data (*Geant4 Physics Reference Manual*), while the low-energy package uses directly the experimental data (Apostolakis *et al* 1999). The PENELOPE package is based on the PENELOPE code (PENetration and Energy LOss of Positrons and Electrons), version 2001 (PENELOPE 2001), where the electron multiple-scattering algorithms of PENELOPE have not yet been implemented.

The energy loss of photons is due to discrete interactions only. The energy loss of electrons, however, is separated into continuous energy loss (soft collisions) and secondary electron production (hard collisions or knock-ons). The production threshold (often referred to as 'cut') is defined as the minimum energy E_{cut} above which secondary particles are produced and tracked. When the electron energy $E < E_{\mathrm{cut}}$, E decreases only by continuous energy loss. When $E > E_{\mathrm{cut}}$, secondary electrons are being produced. This threshold is set as a range cut, internally converted into energy, to avoid the dependence on material.

The user can define four types of cut to limit the tracking of particles: the *maximum total track length*, the *maximum total time of flight*, the *minimum kinetic energy*, and the *minimum remaining range*. When a particle reaches any of these cuts, its remaining energy is deposited locally. Other options (*stepping function*, *maximum allowed step size*, *stepping algorithm*, see Apostolakis *et al* (2009), Agostinelli *et al* (2003), *Geant4 Physics Reference Manual*) are available for controlling the standard electromagnetic processes and allow the user to change the trade-off between accuracy and CPU time. The Geant4 option 3 physics list (*Geant4 Physics Reference Manual*), which has been designed for high-precision simulations in e.g. medical applications, is now available in GATE. The influence of different cut values has been reported upon for not only macro-dosimetry using carbon ions (Zahra *et al* 2010) and protons (Grevillot *et al* 2010a), but also for micro-dosimetry (Frisson *et al* 2009).

3.3. Hadronic processes

Hadronic processes describe the interactions between energetic hadrons/ions and target nuclei. Four main types of nucleon–nucleon collision processes can be distinguished as a function of projectile energy and impact parameter. At low energies, incomplete fusion may occur in central collisions and elastic or inelastic scattering in peripheral collisions. At higher energies, central collisions give rise to fragmentation into several lighter fragments or nucleons, while in peripheral collisions a separation into so-called participant and spectator regions occurs.

In Geant4, fusion, inelastic scattering and fragmentation processes are included in the inelastic process type. Inelastic hadronic interactions allow simulation of the cascade, pre-equilibrium and de-excitation stages of ions interacting with matter. These yield, among other products, prompt-gamma radiations and $\beta+$ emitters. Each process is described through models and sets of interaction data. The different Geant4 models available (Bertini, binary cascade, quantum molecular dynamics model, low-energy parameterized model) offer different levels of complexity for the simulations. Models can be selected as a function of particle type, energy, and material. Most hadronic processes require an explicit choice of models. Several interaction datasets may be available for each hadronic process. The choice of data set as a function of energy is performed with a last-in-first-out method.

GATE does not provide more processes or datasets than the ones available in Geant4, but integrates them for imaging and radiation therapy related applications. Some examples of physics lists are currently provided, based on the Geant4 quark-gluon string precompound—binary cascade (QGSP-BIC) models in the recommended physics list for hadronic interactions. Experienced users can tune any parameter to perform comparisons and choose the options that best describe their data.

4. Modelling of moving sources and generic motion

Moving objects during a simulation is one of the unique original features of GATE compared to other simulation tools used in emission or transmission tomography. This feature is useful for modelling, for instance

- the rotation of image acquisition devices around the patient during acquisition;
- the motion of sources during the simulation, e.g., when the tracer distribution changes during a PET or SPECT acquisition;
- organ motion during SPECT or PET acquisitions;
- CT scans where the x-ray beam performs a complete rotation around the object;
- radiation therapy treatments requiring multiple beam angles to conform the dose to the target.

4.1. Moving sources

The Geant4 architecture is not appropriate for moving or transforming sources during a simulation. Therefore, in previous GATE versions, geometrical (i.e. non-voxelized) sources were moved using the concept of confinement (Jan *et al* 2004). In GATE V6, a new, simple and convenient paradigm is used: each source can be attached to any user-defined geometrical volume. The position and momentum of the source particles are defined relative to the coordinate system of this volume instead of to the world coordinate system. Any source can thus be displaced by moving a geometrical volume with time.

Up to recently, the only way to model dynamic patient processes (due either to changes in radiotracer distribution or in organ positions) in voxelized phantoms was through multiple static simulations corresponding to the patient geometries at fixed time points within a dynamically evolving process (for example respiration, cardiac beating, activity concentration). Although feasible, the problem with this approach was the management of multiple independent simulation processes, which becomes increasingly important when fine temporal sampling of the dynamic process of interest is required.

To facilitate the simulation of complex dynamic processes in the patient, new functionalities have been added to define and manage dynamic voxelized phantoms

(*GateRTPhantom* and *GateRTPhantomMgr*, respectively, where RT stands for real time) (Descourt *et al* 2006). This real-time dynamic phantom simulation approach has been validated in comparison to multiple static simulations at different instances of the respiratory cycle and variable organ time-activity curve simulations using the NCAT voxelized phantom (Segars *et al* 2001, Le Maitre *et al* 2009).

4.2. Modelling motions

A new method for describing complex object motions (*genericMove*) has been introduced in GATE V6. The user can now provide, for each volume of interest, the succession of translations and rotations to be applied as a function of time. Note that the same approach is also used for the *repeater* concept (*genericRepeater*); any volume can now be duplicated at different positions and orientations, at no memory cost, according to a file describing the operations to be followed in the duplication process.

A typical application of these new GATE features is the simulation of intensity modulated radiation therapy (IMRT) treatments. In this application, multiple treatment fields are to be simulated, requiring different beam positions and orientations and different amounts of radiation to be delivered. Moreover, for each beam, a sequence of multi-leaf collimator (MLC) configurations with different time durations is used. GATE now makes it possible to simulate this situation by describing only one leaf that is repeated with the generic repeater and moved according to time. Other applications that require such features are the simulation of arc therapy and other complex treatment systems such as Cyberknife or Tomotherapy devices.

The timing capabilities of GATE have also been enhanced. In GATE, each run is associated with a time slice. Volumes can move in between two time slices only. Simulations can now be split into time slices with durations varying from one time slice to another. According to the source activity, in each time slice a different number of particles can be generated.

5. CT modelling with GATE

CT scanners can be modelled using the CT scanner system. The Geant4 General Particle Source (GPS) allows the user to simulate a realistic x-ray source. Indeed, the GPS can produce particles defined by specific energy, angular and spatial distributions. The energy distribution of the source is defined using an energy histogram (weights against energy bins). The angular distribution is defined using two angles, while the spatial distribution defines the 2D or 3D shape of the source. The CT system is composed of modules that can be linearly repeated along an axis. A module is composed of clusters, each of which corresponds to a set of equally sized pixels (figure 1). This approach enables the modelling of many different types of CT scanner. A complete simulation applies *digitizer* functions at the level of the pixels. The standard output stores 32 bit raw data corresponding to the number of photons detected per CT projection in each pixel. As long as the digitizer model makes sense and is

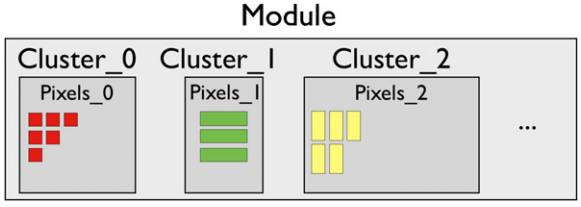

Figure 1. Basic components of the *CT scanner* system.

duly validated against real data, digitizer functions can also be tailored by the user directly at the level of the *module* to avoid time-consuming tracking at the level of the pixels.

6. Variance reduction techniques and other acceleration options

A number of variance reduction techniques (VRTs) appropriate for different types of situations have been introduced in GATE to accelerate simulations. Dedicated publications have already reported and validated the implementation of the regular navigator and fictitious interaction approaches appropriate for SPECT and PET (Rehfeld *et al* 2009), the tabulated modelling of the detector response in SPECT which circumvents the tracking of particles within the collimator/detector pair (Descourt *et al* 2010), and compressed voxel strategies to optimize memory and CPU use (Taschereau and Chatziioannou 2008). In the following, we briefly describe generic VRTs that have recently been added, as well as a simple acceleration option appropriate for CT simulations.

6.1. Classical VRT techniques

Two standard VRTs of Geant4 are now available in GATE, namely splitting and Russian roulette (*Geant4 Physics Reference Manual*). To increase the efficiency of these VR techniques, the user can add selection criteria to be applied to the incident (primary) or secondary particles, using the concept of *filters* (section 2.1). The *filters* for splitting and Russian roulette are the same as those available for *actors*. Using this approach, it is possible to optimize simulations of clinical linear accelerators using selective bremsstrahlung splitting (Kawrakow *et al* 2004).

6.2. Acceleration for CT simulations

To efficiently simulate CT, every photon that reaches the detector surface is split into k clones. Each clone is forced to interact within the CT detector using the direct inversion method, according to the attenuation properties of the detector, and considering the photon cross-section data from the Geant4 standard electromagnetic package. Without acceleration ($k = 1$), the propagation of N photons impinging on the surface of the detector is equivalent to a binomial trial of mean Np, where p is the detection probability. As long as N and p are, respectively, large and small enough, the number of detected photons follows a Poisson distribution of mean and variance equal to Np. Considering the use of k clones, the expectation of the number of detected photons becomes Nkp and its variance is $(Nkp)^2[(k-1)/Nk+1/Nkp]$. As shown in figure 2(a), the relative variance resulting from this acceleration option is perfectly described by this model and increases rapidly when k becomes large. Figure 2(b) shows the acceleration achieved using this approach; obtaining an average count above 10 000 photons/pixel with $k = 10$ clones results in an acceleration of the execution time by a factor around 10 with only a slight increase of the relative variance. Using more clones (e.g. $k = 20$) results in a dramatic increase of the relative variance, although the acceleration factor remains roughly proportional to the number of clones. Indeed, this approach can provide a speedup factor proportional to the number of clones, but it has to be used with caution, since the increase of the relative variance might result in reconstructed images with enhanced noise.

7. Data input and output

It is important that GATE can easily read in data from CT scanners, as such data are often used to design simulations based on realistic patient data, and that it can store data in a format

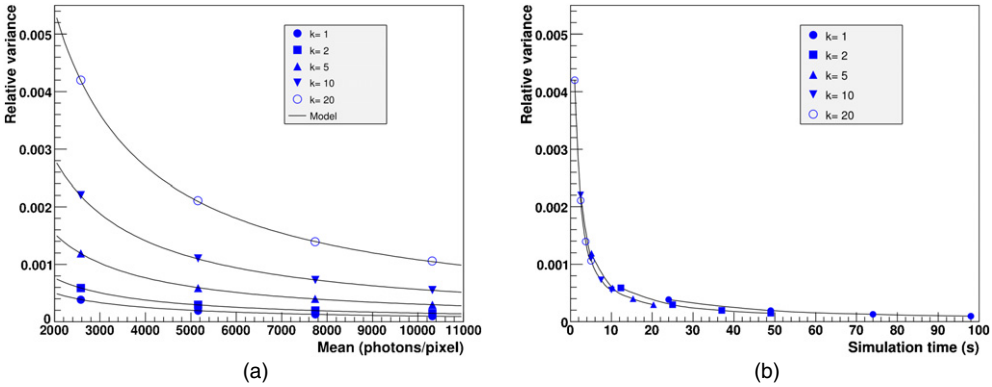

Figure 2. Plot of the relative variance against mean photons/pixel (a) and simulation time (b). The mean and variance of the number of detected photons per pixel are determined from the simulation of a Si pixel detector with 10 000 pixels of 0.5 mm × 0.5 mm × 0.5 mm each irradiated using a flat field of 17.6 keV x-rays. 50 000 realizations were performed to calculate the means and standard deviations. In (a), the relative variance calculated from the simulations is perfectly predicted by the variance given by $(k-1)/Nk+1/Nkp$ derived from the model.

that is readable by other software. New features have been introduced in GATE V6 to comply with these requirements.

7.1. Data input

Using CT images as simulation input requires a method to relate the Hounsfield unit (HU) values in the input image to Geant4 materials. The stoichiometric calibration implemented in GATE V6 is that described by Schneider *et al* (2000). The procedure is based on a user-defined mass density tolerance parameter and two calibration files describing the piecewise linear correspondence between CT numbers and mass density, and a list of material compositions. The tolerance parameter can be used to tune the number of materials depending on the accuracy required in the simulation. The list of materials generated and the correspondence between materials and HU values are stored and can be used for converting any CT image into materials.

7.2. Data output

The *DoseActor* has been added to store 1D, 2D or 3D distributions of dose and/or energy deposited with the associated statistical uncertainty in any volume (Sarrut and Guigues 2008). A user-defined scoring matrix consisting of so-called *dosels* can be attached to any volume, including voxelized geometries. The sizes of the *dosels* can be different from the voxel size (De Smedt *et al* 2005). Every time a particle interacts in the volume, the energy deposited and/or the absorbed dose are recorded in the corresponding *dosel*.

In Geant4, the user has to specify at which location the energy deposited during a *step* is scored, for instance at the beginning or at the end of the *step*. For charged particles, which deposit most of their energy through continuous energy loss, GATE V6 provides a slightly different approach in which the deposited energy is scored at a randomly chosen position along the *step*. This approach ensures that the energy deposited by charged particles is scored correctly on average, even in the vicinity of volume boundaries. Since a *step* is always

interrupted when it crosses a volume boundary, other dose scoring methods may introduce biases.

The *DoseActor* is compatible with variance reduction techniques as the deposited energy is weighted by the particle weight. In addition to the deposited energy, an estimation of the relative statistical uncertainty is computed as proposed by Chetty *et al* (2006). When a simulation is split into multiple jobs, such as when using clusters of workstations, the total uncertainty cannot be computed directly from the uncertainties obtained for each job. In this case the first and second moment of the energy distribution are stored for each job and the uncertainty can be calculated retrospectively.

7.3. Phase-space files

GATE V6 allows the user to record so-called phase-space files containing the essential properties of the simulated particles at a given geometric level.

For imaging applications, particle tracking can be limited to the phantom (or patient). The properties of each particle exiting the phantom are stored in a phase-space file. This output file can then be used as an input file in subsequent GATE simulations (or even in other software), in which the stored particles are further propagated towards the detector. This option can be useful to efficiently study or optimize different detector set-ups, since the simulation of particles within the phantom has to be performed only once.

For radiotherapy applications, the phase-space file can be used, for instance, to first simulate the linear-accelerator head (patient-independent part) and then store the properties of the particles before they enter the MLC. The phase space can subsequently be used to simulate different treatment scenarios (patient-dependent part). In this case, phase-space files are created using an actor (*phaseSpaceActor*) that collects the relevant properties of all particles passing through a given region. The particle properties that can be stored are the energy, type, position, direction, weight, and the process and volume of production. The phase-space data can be stored in ROOT or in a standard IAEA format (Capote *et al* 2006). The IAEA format can be used to produce phase-space files for other MC codes. Conversely, an IAEA file produced by another code can be used in a GATE simulation that considers all particles in the phase-space file as primary particles.

8. New GATE V6 benchmark

GATE benchmarks provide users with relatively easy simulation set-ups that can be run with any GATE release to check the validity of the user's results by comparing them with the results provided on the GATE website and to track changes between versions. A new benchmark related to radiation therapy applications is distributed with GATE V6.

The radiotherapy benchmark consists of a proton beam and a photon beam interacting in a 40 cm $\times$ 40 cm $\times$ 40 cm water phantom. The beam energy is set to 150 MeV for the proton beam and to 18 MV for the photon beam. The physics list used in this benchmark is that recommended by the Geant4 collaboration for the hadrontherapy applications (https://twiki.cern.ch/twiki/bin/view/Geant4/LowePhysicsLists). Three hundred and fifty thousand protons and 2 million photons are generated. The total computing time for this benchmark is about 1 h on an Intel Xeon 5130 CPU at 2.0 GHz.

The simulated energy deposition profile is shown in figure 3. This figure is automatically produced by the analysis code provided with the benchmark. A statistics file containing the number of events, tracks, and steps is also generated. Table 1 shows the mean values and the associated standard deviations obtained by running the benchmark with GATE V6.1 on four

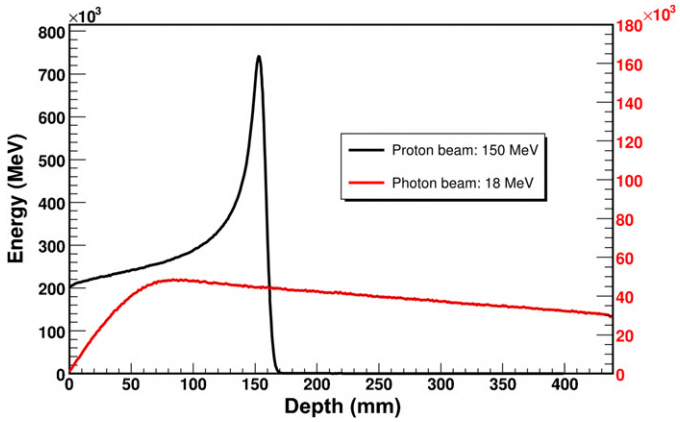

Figure 3. Energy deposition profiles obtained when running the radiation therapy benchmark.

Table 1. Average values ± 1 standard deviation of parameters analysed in the radiation therapy benchmark.

Beam	Number of events	Number of tracks	Number of steps	Number of geometric steps	Number of physical steps
Protons (150 MeV)	350 000	17 851 294 ± 100 047	105 566 062 ± 293 928	588 828 ± 4221	104 977 233 ± 297 892
Photons (18 MV)	2 000 000 ± 0	34 191 416 ± 44 709	127 354 486 ± 173 392	8 166 686 ± 3621	119 187 800 ± 169 779

different sites. These values serve as reference values for checking the integrity of a GATE installation and to track changes from one GATE version to another.

9. Preliminary validation results for radiation therapy applications

The ICRU (1993) definition was used for all materials involved in the studies reported in this section (composition, density, ionization potential).

9.1. Photon beam radiation therapy

A realistic photon beam in a multilayer phantom was modelled. The phantom (30.5 × 39.5 × 30 cm^3) consisted of four layers: water (0–3 cm), aluminium (3–5 cm), lung (5–12 cm) and water (12–30 cm). The phantom was irradiated with a 18 MV photon beam, originating from a uniform point source at 100 cm from the phantom surface and collimated to 1.5 × 1.5 cm^2 at the surface of the phantom using four *KillActors*. The energy spectrum of the point source fitted the configurations of a VARIAN Clinac 2100C as modelled using the BEAM code (Rogers *et al* 1995). The depth–dose distribution was calculated along the central axis with a 1D *DoseActor*. The *dosel* dimensions were 5 mm × 5 mm orthogonally to the beam direction and 2 mm along the beam direction. We used the standard physics list with option 3 (see section 3) for electrons, positrons and photons. The production threshold was set to 1 mm in the world and to 0.1 mm in the phantom for electrons, positrons and photons. A total

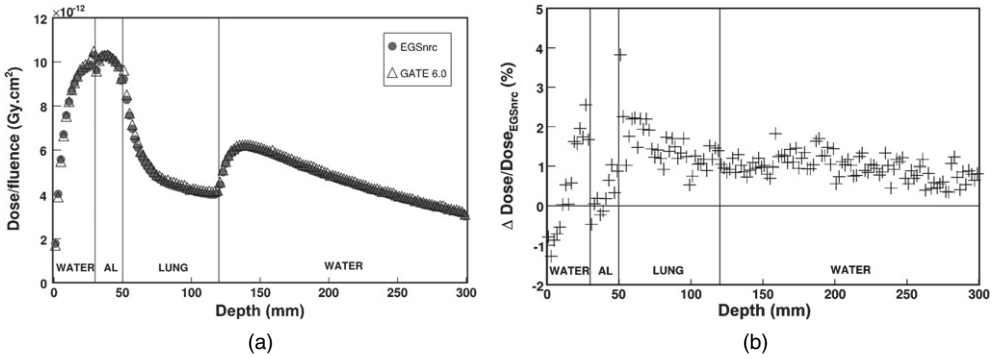

Figure 4. (a) Dose deposited per unit photon fluence as a function of depth in a multilayer phantom for an 18 MV photon beam. Results with GATE V6.0 (open diamonds) are compared with results with EGSnrc (black circles). (b) Relative differences d_r between the depth–dose distributions calculated with EGSnrc and GATE.

of 10^8 incident photons were simulated. The statistical relative uncertainty was below 0.6% in all dosels.

The depth–dose profile calculated with GATE was compared to that obtained with EGSnrc following the configuration reported by Rogers and Mohan (2000) using the PRESTAII stepping algorithm (figure 4). Two relative differences in dose estimates were derived: $d_r = (\text{Dose}_{\text{GATE}} - \text{Dose}_{\text{EGS}})/\text{Dose}_{\text{EGS}}$ and $d_m = (\text{Dose}_{\text{GATE}} - \text{Dose}_{\text{EGS}})/\text{Dose}_{\text{max}}$, where $\text{Dose}_{\text{GATE}}$, Dose_{EGS} and Dose_{max} are the dose values calculated by GATE, EGSnrc, and max($\text{Dose}_{\text{GATE}}$, Dose_{EGS}), respectively. The results obtained using GATE V6 were in good agreement with EGSnrc results, with d_r less than 3% and d_m less than 1.8%. The computation time was about 3 h on an Intel 2.3 GHz CPU.

9.2. Electron beam radiation therapy

A realistic 20 MeV electron beam was modelled in a multilayer phantom (30.5 cm × 39.5 cm × 8 cm) consisting of four layers: water (0–2 cm), aluminium (2–3 cm), lung (3–6 cm) and water (6–8 cm). A total of 2.5×10^5 electrons were simulated. The *dosel* dimensions were 5 mm × 5 mm orthogonally to the beam direction and 2 mm along the beam direction. The statistical relative uncertainty increased from 0.6% near the phantom entrance surface to 2.6% near the exit surface.

The depth–dose distribution obtained with GATE was compared to the results obtained using EGSnrc following the configuration reported in Rogers and Mohan (2000) using the PRESTAII stepping algorithm (figure 5). The d_r and d_m relative dose differences defined in section 9.1 were calculated. GATE V6.0 yielded results in good agreement with EGSnrc results with d_r less than 4% (except at 8 cm where d_r reaches 7.5% with a statistical uncertainty of ∼7%) and d_m less than 1.1%. The computation time was about 6 h on an Intel 2.3 GHz CPU.

9.3. Proton beam radiation therapy

The depth–dose profile of a 150 MeV mono-energetic proton beam in a 40 cm × 40 cm × 40 cm water phantom was calculated. The proton beam had a Gaussian fluence profile with a

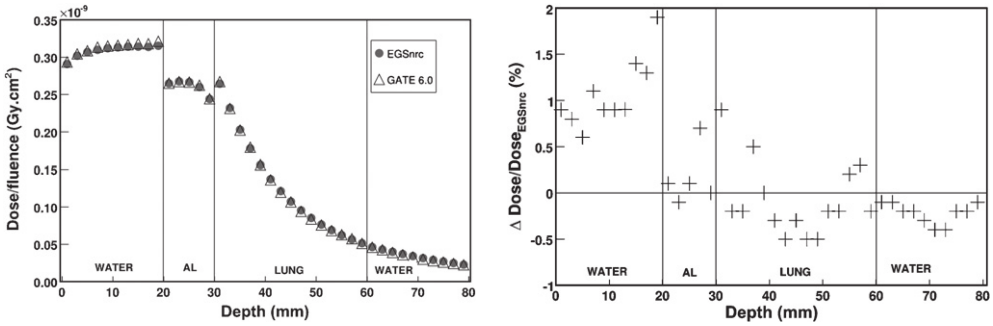

Figure 5. (a) Dose deposited per unit electron fluence as a function of depth in the multilayer phantom for a 20 MeV mono-energetic electron beam. Results with GATE V6.0 (open diamonds) are compared with EGSnrc (black circles). (b) Relative differences d_r between the depth–dose distributions calculated with EGSnrc and GATE.

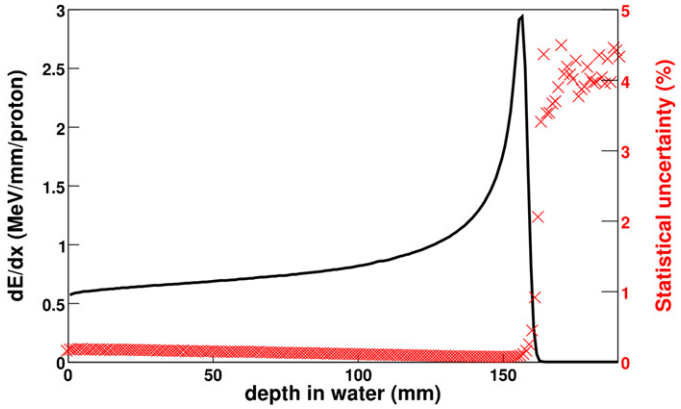

Figure 6. Normalized energy deposited by a 150 MeV proton beam as a function of depth in water (black curve, left-hand axis) and associated relative statistical uncertainty (red curve, right-hand axis).

standard deviation of 3 mm. The *dosel* dimensions were 40 cm × 40 cm orthogonally to the beam and 1 mm along the beam direction. The *hadrontherapyStandardPhys.mac* physics list proposed in GATE was used, with an additional *StepLimiter* of 1 mm and default production thresholds (1 mm range cut for electrons, positrons and photons). A total of 10^6 incident protons were simulated in 57 min on a single 1.66 GHz CPU.

The results shown in figure 6 show that the relative statistical uncertainty is below 0.1% for all dosels before the distal tail of the Bragg peak (oscillations after the peak are due to the near-zero values of deposited energy at the corresponding depths). The proton range, defined as the position of 80% of the maximum dose in the distal fall-off region, is 158 mm. This agrees to within 0.3 mm with the CSDA range of 157.7 mm given by the NIST PSTAR database (http://physics.nist.gov/PhysRefData/Star/Text/PSTAR.html). The peak-to-entrance energy ratio, defined as the ratio between the maximum dose and the dose in the entrance dosel, is 5.15. The peak width, defined as the distance between the points at which the dose equals 80% of the maximum dose at either side of the Bragg peak, is 5.5 mm.

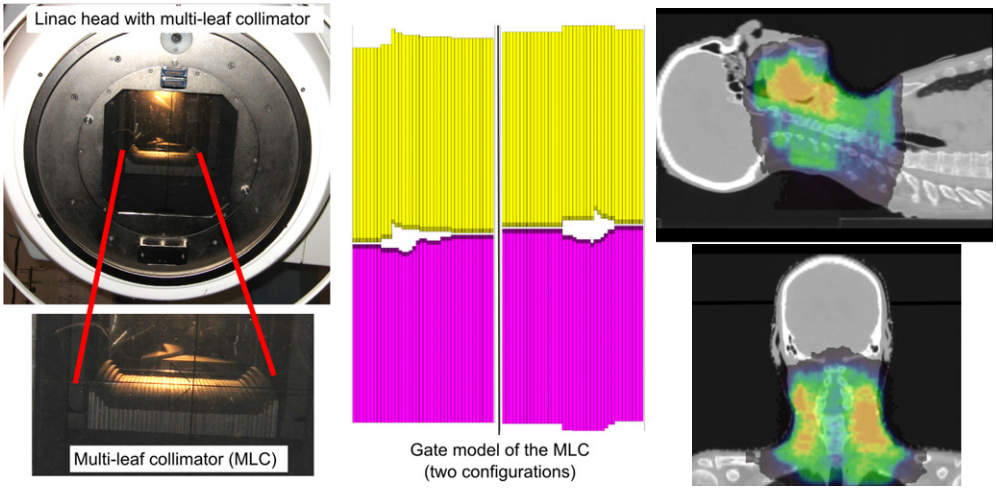

Figure 7. A multi-leaf collimator (a) and two of its modelled configurations (b) during an IMRT treatment plan simulated with GATE. The resulting dose distribution (c) is superimposed on two CT slices.

10. Examples of GATE V6 simulations

10.1. Radiation therapy examples

To illustrate a radiotherapy application of GATE, we exported a head and neck IMRT treatment plan from a XIO (CMS) treatment planning system and converted it into GATE macros. The plan was composed of 5 beams with 20 leaf positions, simulated using 100 GATE runs. The MLC was simulated by describing a single leaf and using the *genericMove* and *genericRepeater* as discussed in section 4.2 (figure 7). The DICOM data of the patient CT scan were converted into a GATE readable file format (Analyze), using the stoichiometric calibration described in section 7. This 3D dose simulation (10^9 particles in about 33 h on a single Intel 2.7 GHz CPU) has not yet been compared to TPS results nor to experimental measurements. Our primary goal here was to illustrate that complex simulations including voxelized phantoms, MLC models, and motion were feasible with GATE. The relative statistical uncertainty is lower than 1% in the high-dose region (i.e. where the dose is $> 50\%$ of the maximum dose).

As an example of a hadron therapy application, we simulated a ^{12}C scanning pencil beam irradiation of an artificial spherical target inside a patient CT image. The treatment plan comprised 12×12 spots at 24 different energy layers ($\sim$3500 different pencil beams of which $\sim$2200 with non-zero intensity). The beams were described according to the results of a spread-out Bragg peak (SOBP) optimization performed with the method of Krämer *et al* (2000). Ion ranges were estimated using the water equivalent path length obtained from the CT numbers (Krämer *et al* 2000). The biological dose was estimated using the method of Kase *et al* (2006). Figure 8 illustrates the dose deposition measured using this simulation, which took $\sim$15 min on a one hundred AMD Opteron 2.3 GHz CPU cluster.

10.2. In-beam PET modelling with GATE

To illustrate the ability of GATE to jointly model radiation therapy and emission tomography, a complete in-beam PET set-up was simulated. A 4D CT patient scan was used to define

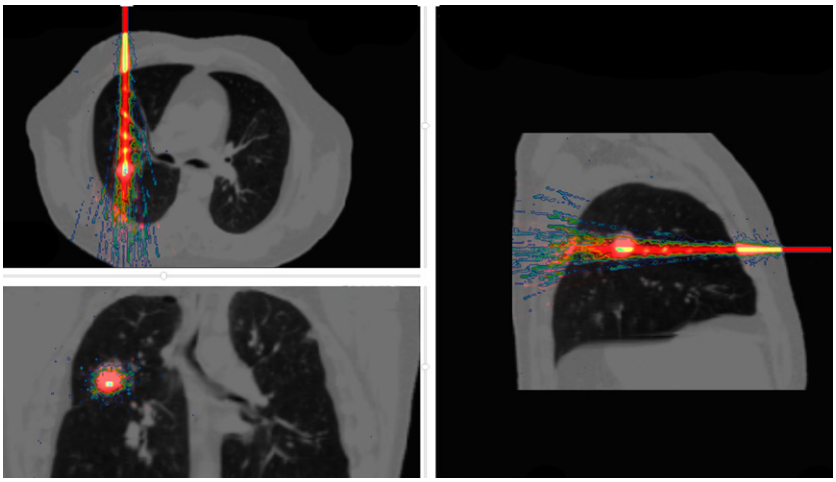

Figure 8. Dose deposited by a carbon ion beam inside a CT image of a thorax. The colour scale is a warm metal scale, with high values (white) corresponding to high-dose deposit and low values (blue) corresponding to low-dose deposit.

the numerical phantom. A three-beam treatment plan was modelled with a total production of 3×10^9 ^{12}C ions. Each beam was composed of 195 independent spots with 42 different incident energies between 175 and 230 MeV/u. All hadronic and electromagnetic processes were included in the simulation, from the ^{12}C ion tracking to the β^+ decay of ^{11}C and ^{15}O produced by nuclear reactions. Positron range and annihilation photon pair acollinearity were taken into account. A model of the Siemens HR+ PET system (Jan *et al* 2005) was used to simulate a 20 min static acquisition starting immediately after the ^{12}C irradiation. PET data were normalized, corrected for attenuation using an attenuation map derived from the CT, and reconstructed using 3D back projection. The simulation was performed in less than 24 h on a cluster of 1000 Intel Nehalem 2.93 GHz CPUs.

The reconstructed PET images (figure 9) suggest that the ^{11}C activity distribution (mainly created by auto-activation) contains most information regarding the location of the SOBP, while the ^{15}O activity (entirely due to target activation) might be relevant to derive information about the dose to normal tissues.

10.3. Example of CT modelling with GATE

As an example, we have tentatively simulated the design of the XPAD3 hybrid pixel detector, a prototype x-ray photon counting detector under development at CPPM (Nicol *et al* 2009) operated with a source emitting a cone beam of x-rays of 12° aperture angle with a typical Mo target energy spectrum. The x-ray detector was composed of five barrettes of seven chips of 80×120 pixels tiled together, corresponding to 336 000 500 μm thick pixels of 130×130 μm^2. The 4D MOBY phantom was used with $435 \times 435 \times 600$ voxels of 60 μm (Segars *et al* 2004). A total of 25 279 488 photons were detected per time slice of 1 s. The complete simulation took 149 min on an Intel Core 2 Duo T9600 processor operating at 2.80 GHz. It took only 14 min with the acceleration option using 10 clones.

Figure 10 shows two cone-beam projections of the MOBY phantom simulated without (figure 10(a)) and with (figure 10(b)) the acceleration option. The projections are shown as

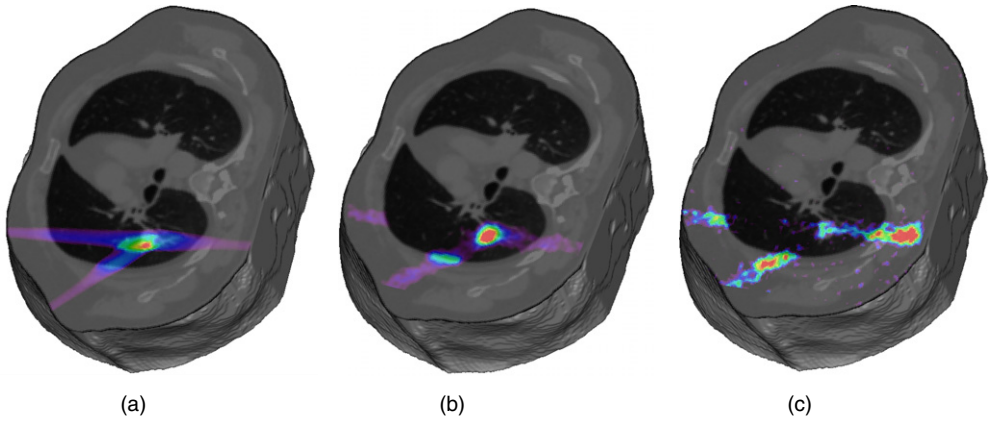

Figure 9. (a) Dose distribution simulated for a ^{12}C irradiation inside a CT image of a thorax. (b) Simulated PET image of the resulting ^{11}C isotope distribution. (c) Simulated PET image of the ^{15}O isotope distribution.

matrices filled with the raw counts of the pixels and do not reproduce the actual geometry of the detector with its tiles. 360 projections per scan are used to reconstruct an image using the FDK algorithm while taking into account the actual geometry of the detector (figure 10(c)). The image reconstructed with projections using the acceleration option with ten clones (figure 10(d)) does not show any structured artefacts but appears of poorer quality compared to the image without the acceleration option, due to the increased variance in the projections.

This example is not intended to be a validation of the CT model but illustrates the feasibility of CT simulations with GATE at a reasonable computational cost.

11. Discussion

The broad use of GATE in detector design, imaging and processing protocol optimization, and even in image reconstruction, motivated the enhancements described in this paper. Based on its new features, GATE should meet the needs of an increasing number of scientists involved in SPECT, PET and CT imaging, and now also in external beam photon and hadron radiotherapy. An important consequence of the use of the same software by many scientists is that it makes it easier to compare, share and understand results.

Of course, this also makes it important that the software is thoroughly validated. GATE has already been validated for a number of PET and SPECT imaging configurations by comparing simulated and experimental data (Lazaro *et al* 2004, Staelens *et al* 2003, Gonias *et al* 2007, Van Der Laan *et al* 2007, Rey *et al* 2007, Karakatsanis *et al* 2006, Lamare *et al* 2006, Schmidtlein *et al* 2006, Visvikis *et al* 2006b, Chung *et al* 2005, Assié *et al* 2005, Jan *et al* 2005, Cassol Brunner *et al* 2009, Chen *et al* 2009). For radiation therapy, the relevant Geant4 models have already been partly studied (Carrier *et al* 2004, Pshenichnov *et al* 2005, 2006, Jiang *et al* 2004, Paganetti 2004, Jarlskog and Paganetti 2008). More extensive validation of GATE V6 and underlying Geant4 models for proton and ion therapy applications is currently ongoing.

Upon completion of these validation studies, GATE V6 will provide a unique tool for simulations involving both radiotherapy and imaging. Examples of approaches in which imaging and therapy are integrated include the use of PET imaging to delineate the

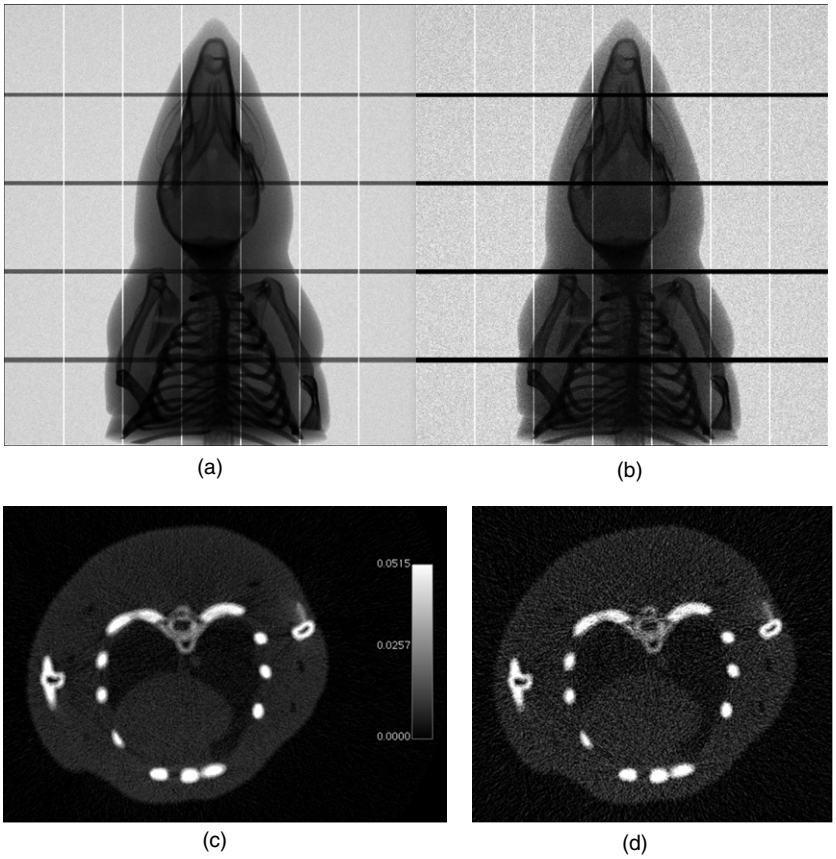

Figure 10. Example of a simulated CT projection of a Moby phantom: without ($k = 1$) (a) and with acceleration ($k = 10$ clones) (b). Transaxial slices reconstructed from the projections without (c) and with acceleration (d).

metabolically active tumour to be irradiated (Ford *et al* 2009), online imaging in external beam therapy, ranging from portal imaging (EPIDs) (van Elmpt *et al* 2008) and integrated x-ray imaging (Mutanga *et al* 2007, Sonke *et al* 2009) to e.g. the Cyberknife (Seppenwoolde *et al* 2007) and Tomotherapy devices (Welsh *et al* 2004), the emerging domain of in-beam imaging in proton and ion therapy (Crespo *et al* 2007, Knopf *et al* 2008, Nishio *et al* 2006, Parodi *et al* 2008), and targeted radiotherapy using radionuclides that can also be imaged (e.g., Kwekkeboom *et al* 2000, Seevinck *et al* 2007). Each of these applications may benefit from the availability of an integrated software supporting both imaging and radiation therapy simulations.

In addition to the recent developments of GATE towards radiotherapy applications, the extension of GATE to optical imaging is also in progress. Optical imaging is of growing importance in the field of preclinical imaging. However, most optical acquisitions are currently limited to 2D projections, without any quantitative analysis of the resulting images. Simulations may help in the design of devices for 3D quantitative optical imaging and associated reconstruction algorithms accounting for optical scattering in tissues. To date, although several approaches have been described in the literature (Wang *et al* 1995, Boas *et al*

2002, Li *et al* 2004), there is no commonly accepted software to perform such simulations. Extending GATE to optical imaging requires us to integrate the relevant physics processes, add databases containing the optical properties of different tissues and materials, and add systems and digitizer options relevant to optical imaging devices.

A weakness of previous GATE versions that many users are aware of is its relatively low computational efficiency. Several options have recently been introduced to speed up GATE in specific situations (section 6) and better manage the trade-off between computation time and accuracy. However, additional options may be worth investigating, especially for applications such as the calculation of system matrices for tomographic image reconstruction (Rehfeld *et al* 2010). Furthermore, the possibility of running GATE on hybrid CPU/GPU architectures is currently under study. At the same time, tools to facilitate the deployment of GATE on grids are being developed (Camarasu *et al* 2010).

Several computer-oriented developments other than those described here have been introduced to facilitate the use of GATE by users and developers, such as the distribution of GATE as an image appropriate for virtual machines, providing the documentation as a wiki, etc. All of these developments aim at making GATE accessible to scientists involved in SPECT, PET, CT and radiotherapy applications, without requiring expertise in computer science or C++ programming.

12. Conclusion

The introduction of a large number of new features in GATE V6 now makes it possible to use GATE as an integrated tool for the modelling of imaging, dosimetry and treatment in the same simulation platform, consistent with current and future needs of the nuclear medicine and radiation therapy communities. Extensive validation studies are currently being performed to establish the role of GATE in the development of image-guided radiation therapy.

References

Agostinelli *et al* 2003 Geant4—a simulation toolkit *Nucl. Instrum. Methods Phys. Res.* **506** 250–303

Apostolakis J, Giani S, Maire M, Nieminen P, Pia M G and Urban 1999 Geant4 low energy electromagnetic models for electrons and photons CERN-OPEN-99-034, INFN/AE-99/18

Apostolakis J *et al* 2009 Geometry and physics of the Geant4 toolkit for high and medium energy applications *Rad. Phys. Chem.* **78** 859–73

Assié K, Gardin I, Vera P and Buvat I 2005 Validation of the Monte Carlo simulator GATE for Indium 111 imaging *Phys. Med. Biol.* **50** 3113–25

Boas D, Culver J, Stott J and Dunn A 2002 Three dimensional Monte Carlo code for photon migration through complex heterogeneous media including the adult human head *Opt. Express* **10** 159–70

Bruyndonckx P, Lemaître C, Schaart D R, van Der Laan D J, Maas M C, Krieguer M, Devroede O and Tavernier S 2007 Towards a continuous crystal APD-based PET detector design *Nucl. Instrum. Methods Phys. Res.* A **571** 182–6

Camarasu-Pop S, Glatard T, Mościcki J T, Benoit-Cattin H and Sarrut D 2010 Dynamic partitioning of GATE Monte-Carlo simulations on EGEE *J. Grid Comput.* **8** 241–59

Capote R, Jeraj R, Ma C P, Rogers D W O, Sanchaez-Doblado F, Sempau J, Seuntjens J and Siebers J V 2006 Phase-space database for external beam radiotherapy *IAEA Technical Report* INDC(NDS)-0484

Carrier J F, Archambault L, Beaulieu L and Roy R 2004 Validation of Geant4, an object-oriented Monte Carlo toolkit, for simulations in medical physics *Med. Phys.* **31** 484–92

Cassol Brunner F, Khoury R, Benoit D, Meessen C, Bonissent A and Morel C 2009 Simulation of PIXSCAN, a photon counting micro-CT for small animal imaging *J. Instrum.* **4** P05012

Chen Y, Liu B, O'Connor J M, Didier C S and Glick S J 2009 Characterization of scatter in cone-beam CT breast imaging: comparison of experimental measurements and Monte Carlo simulation *Med. Phys.* **36** 857–69

Chetty I J *et al* 2006 Reporting and analyzing statistical uncertainties in Monte Carlo-based treatment planning *Inter. J. Radiat. Oncol. Biol. Phys.* **65** 1249–59

Chung Y H, Choi Y, Cho G S, Choe Y S, Lee K H and Kim B T 2005 Optimization of dual layer phoswich detector consisting of LSO and LuYAP for small animal PET *IEEE Trans. Nucl. Sci.* **52** 217–21

Crespo P, Shakirin G, Fiedler F, Enghardt W and Wagner A 2007 Direct time-of-flight for quantitative, real-time in-beam PET: a concept and feasibility study *Phys. Med. Biol.* **52** 6795–811

De Beenhouwer J, Staelens S, Kruecker D, Ferrer L, D'Asseler Y, Lemahieu I and Rannou F R 2007 Cluster computing software for GATE simulations *Med. Phys.* **34** 1926–33

De Beenhouwer J, Staelens S, Vandenberghe S and Lemahieu I 2008 Acceleration of GATE SPECT simulations *Med. Phys.* **35** 1476–85

Descourt P, Carlier T, Du Y, Song X, Buvat I, Frey E C, Bardies M, Tsui B M W and Visvikis D 2010 Implementation of angular response function modeling in SPECT simulations with GATE *Phys. Med. Biol.* **55** N253–66

Descourt P, Segars W P, Lamare F, Ferrer L, Tsui B, Bizais Y, Bardies M and Visvikis D 2006 RTNCAT (Real Time NCAT): implementing real time physiological movement of voxellised phantoms in GATE *IEEE Nucl. Sci. Symp. Conf. Rec.* pp 3163–5

De Smedt B, Vanderstraeten B, Reynaert N, De Neve W and Thierens H 2005 Investigation of geometrical and scoring grid resolution for Monte Carlo dose calculations for IMRT *Phys. Med. Biol.* **50** 4005–19

Ferrer L, Chouin B, Bitar A, Lisbona A and Bardies M 2007 Implementing dosimetry in GATE: dose point kernel validation with GEANT4 4.8.1 *Cancer Biother. Radiopharm.* **22** 125–9

Ford E C, Herman J, Yorke E and Wahl R L 2009 18F-FDG PET/CT for image-guided and intensity-modulated radiotherapy *J. Nucl. Med.* **50** 1655–65

Frisson T, Zahra N, Lautesse P and Sarrut D 2009 Monte-Carlo based prediction of radiochromic film response for hadrontherapy dosimetry *Nucl. Instrum. Methods Phys. Res.* A **606** 749–54

Geant4 Collaboration *Geant4 Physics Reference Manual* http://geant4.cern.ch/G4UsersDocuments/UsersGuides/PhysicsReferenceManual/html/PhysicsReferenceManual.html

Gonias P *et al* 2007 Validation of a GATE model for the simulation of the Siemens PET/CT biograph 6 scanner *Nucl. Instrum. Methods Phys. Res.* A **571** 263–6

Grevillot L, Frisson T, Zahra N, Bertrand D, Stichelbaut F, Freud N and Sarrut D 2010a Optimization of GEANT4 settings for proton pencil beam scanning simulations using GATE *Nucl. Instrum. Methods Phys. Res.* B **268** 3295–305

Grevillot L, Frisson T, Maneval D, Zahra N, Badel J-N and Sarrut D 2010b Simulation of a 6 MV Elekta Precise Linac photon beam using GATE/GEANT4 *Phys. Med. Biol.* **56** 903–18

ICRU 1993 Stopping Powers and Ranges for Protons and Alpha Particles *ICRU Report No 49* (Bethesda, MD: ICRU)

Jan S *et al* 2004 GATE: a simulation toolkit for PET and SPECT *Phys. Med. Biol.* **49** 4543–61

Jan S, Comtat C, Strul D, Santin G and Trébossen R 2005 Monte Carlo simulation for the ECAT EXACT HR+ system using GATE *IEEE Trans. Nucl. Sci.* **52** 627–33

Janecek M and Moses W W 2010 Simulating scintillator light collection using measured optical reflectance *IEEE Trans. Nucl. Sci.* **57** 964–70

Jarlskog C Z and Paganetti H 2008 Physics settings for using the Geant4 toolkit in proton therapy *IEEE Trans. Nucl. Sci.* **55** 1018–25

Jiang H and Paganetti H 2004 Adaptation of GEANT4 to Monte Carlo dose calculations based on CT data *Med. Phys.* **31** 2811–8

Karakatsanis N *et al* 2006 Comparative evaluation of two commercial PET scanners, ECAT EXACT HR+ and Biograph 2, using GATE *Nucl. Instrum. Methods Phys. Res.* A **571** 368–72

Kase Y, Kanematsu N, Kanai T and Matsufuji N 2006 Biological dose calculation with Monte Carlo physics simulation for heavy-ion radiotherapy *Phys. Med. Biol.* **51** N467–75

Kawrakow I, Rogers D W and Walters B R 2004 Large efficiency improvements in BEAMnrc using directional bremsstrahlung splitting *Med. Phys.* **31** 2883–98

Knopf A, Parodi K, Paganetti H, Cascio E, Bonab A and Bortfeld T 2008 Quantitative assessment of the physical potential of proton beam range verification with PET/CT *Phys. Med. Biol.* **53** 4137–51

Krämer M, Jäkel O, Haberer T, Kraft G, Schardt D and Weber U 2000 Treatment planning for heavy-ion radiotherapy: physical beam model and dose optimization *Phys. Med. Biol.* **45** 3299–317

Kwekkeboom D, Krenning E P and de Jong M 2000 Peptide receptor imaging and therapy *J. Nucl. Med.* **41** 1704–13

Lamare F, Turzo A, Bizais Y, Le Rest C C and Visvikis D 2006 Validation of a Monte Carlo simulation of the Philips Allegro/GEMINI PET systems using GATE *Phys. Med. Biol.* **51** 943–62

Lazaro D *et al* 2004 Validation of the GATE Monte Carlo simulation platform for modelling a CsI(Tl) scintillation camera dedicated to small-animal imaging *Phys. Med. Biol.* **49** 271–85

Le Maitre A, Segars W P, Marache S, Reilhac A, Hatt M, Tomei S, Lartizien C and Visvikis D 2009 Incorporating patient specific variability in the simulation of realistic whole body 18F-FDG distributions for oncology applications *Proc. IEEE* **97** 2026–38

Levin A and Moisan C 1996 A more physical approach to model the surface treatment of scintillation counters and its implementation into DETECT *IEEE Nucl. Sci. Symp. Conf. Rec.* **2** 702–6

Li H *et al* 2004 A mouse optical simulation environment (MOSE) to investigate bioluminescent phenomena in the living mouse with the Monte Carlo method *Acad. Radiobiol.* **11** 1029–38

Mutanga T F, de Boer H C J, van der Wielen G J, Wentzler D, Barnhorn J, Incrocci L and Heijmen B J M 2007 Stereographic targeting in prostate radiotherapy: speed and precision by daily automatic positioning corrections using kilovoltage/megavoltage image pairs *Int. J. Radiat. Oncol. Biol. Phys.* **71** 1074–83

Nicol S *et al* 2009 Design and construction of the ClearPET/XPAD small animal PET/CT scanner *IEEE Nucl. Sci. Symp. Conf. Rec.* pp 3311–4

Nishio T, Ogino T, Nomura K and Uchida H 2006 Dose-volume delivery guided proton therapy using beam on-line PET system *Med. Phys.* **33** 4190–7

Paganetti H 2004 Four-dimensional Monte Carlo simulation of time-dependent geometries *Phys. Med. Biol.* **49** N75–81

Parodi K, Bortfeld T and Haberer T 2008 Comparison between in-beam and offline positron emission tomography imaging of proton and carbon ion therapeutic irradiation at synchrotron- and cyclotron-based facilities *Int. J. Radiat. Oncol. Biol. Phys.* **71** 945–56

PENELOPE 2001 PENELOPE: a code system for Monte Carlo simulation of electron and photon transport *Workshop Proc. Issy-les-Moulineaux (AEN-NEA, France, 5–7 November 2001)*

Pshenichnov I, Mishustin I and Greiner W 2005 Neutrons from fragmentation of light nuclei in tissue-like media: a study with the GEANT4 toolkit *Phys. Med. Biol.* **50** 5493–507

Pshenichnov I, Mishustin I and Greiner W 2006 Distributions of positron-emitting nuclei in proton and carbon-ion therapy studied with GEANT4 *Phys. Med. Biol.* **51** 6099–112

Rehfeld N, Vauclin S, Stute S and Buvat I 2010 Multidimensional B-spline parameterization of the detection probability of PET systems to improve the efficiency of Monte Carlo simulations *Phys. Med. Biol.* **55** 3339–61

Rehfeld N S, Stute S, Apostolakis J, Soret M and Buvat I 2009 Introducing improved voxel navigation and fictitious interaction tracking in GATE for enhanced efficiency *Phys. Med. Biol.* **54** 2163–78

Rey M, Jan S, Vieira J M, Mosset J B, Krieguer M, Comtat C and Morel C 2007 Count rate performance study of the Lausanne ClearPET scanner demonstrator *Nucl. Instrum. Methods* A **571** 207–10

Rogers D and Mohan R 2000 Questions for comparison of clinical Monte Carlo codes *13th Int. Conf. on the Use of Computers in Radiation Therapy* ed W Schlegel and T Bortfeld (Heidelberg: Springer) pp 120–2

Rogers D W O, Faddegon B A, Ding G X, Ma C M, We J and Mackie T R 1995 BEAM: a Monte Carlo code to simulate radiotherapy treatment units *Med. Phys.* **22** 503–24

Santin G, Strul D, Lazaro D, Simon L, Krieguer M, Vieira Martins M, Breton V and Morel C 2003 GATE, a Geant4-based simulation platform for PET and SPECT integrating movement and time management *IEEE Trans. Nucl. Sci.* **50** 1516–21

Sarrut D and Guigues L 2008 Region-oriented CT image representation for reducing computing time of Monte Carlo simulations *Med. Phys.* **35** 1452–63

Schmidtlein C R *et al* 2006 Validation of GATE Monte Carlo simulations of the GE Advance/Discovery LS PET scanner *Med. Phys.* **33** 198–208

Schneider W, Bortfeld T and Schlegel W 2000 Correlation between CT numbers and tissue parameters needed for Monte Carlo simulations of clinical dose distributions *Phys. Med. Biol.* **45** 459–78

Seevinck P R, Seppenwoolde J H, de Wit T C, Nijsen J F W, Beekman F J, van het Schip A D and Bakker C J G 2007 Factors affecting the sensitivity and detection limits of MRI, CT, and SPECT for multimodal diagnostic and therapeutic agents anti-cancer agent *Med. Chem.* **7** 317–34

Segars W P, Lalush D S and Tsui B M W 2001 Modeling respiratory mechanics in the MCAT and spline-based MCAT phantoms *IEEE Trans. Nucl. Sci.* **48** 89–97

Segars W P, Tsui B M W, Frey E C, Johnson G A and Berr S S 2004 Development of a 4-D digital mouse phantom for molecular imaging research *Mol. Imag. Biol.* **6** 149–59

Seppenwoolde Y, Berbeco R I, Nishioka S, Shirato H and Heijmen B 2007 Accuracy of tumor motion compensation algorithm from a robotic respiratory tracking system: a simulation study *Med. Phys.* **34** 2774–84

Sonke J J, Rossi M, Wolthaus J, van Herk M, Damen E and Belderbos J 2009 Frameless stereotactic body radiotherapy for lung cancer using four-dimensional cone beam CT guidance *Int. J. Radiat. Oncol. Biol. Phys.* **74** 567–74

Staelens S, De Beenhouwer J, Kruecker D, Maigne L, Rannou F, Ferrer L, D'Asseler Y, Buvat I and Lemahieu I 2006 GATE: improving the computational efficiency *Nucl. Instrum. Methods Phys. Res.* A **569** 341–5

Staelens S, Strul D, Santin G, Vandenberghe S, Koole M, D'Asseler Y, Lemahieu I and Van de Walle R 2003 Monte Carlo simulations of a scintillation camera using GATE: validation and application modelling *Phys. Med. Biol.* **48** 3021–42

Taschereau R and Chatziioannou A F 2007 Monte Carlo simulations of absorbed dose in a mouse phantom from 18-fluorine compounds *Med. Phys.* **34** 1026–36

Taschereau R and Chatziioannou A F 2008 Compressed voxels for high-resolution phantom simulations in GATE *Mol. Imaging Biol.* **10** 40–7

Thiam C O, Breton V, Donnarieix D, Habib B and Maigne L 2008 Validation of a dose deposited by low energy photons using GATE/GEANT4 *Phys. Med. Biol.* **53** 3039–55

Van Der Laan D J, Maas M C, de Jong H W A M, Schaart D R, Bruyndonckx P, Lemaitre C and van Eijk C W E 2007 Simulated performance of a small-animal PET scanner based on monolithic scintillation detectors *Nucl. Instrum. Methods Phys. Res.* A **571** 227–30

Van Der Laan D J, Maas M C, Schaart D R, Bruyndonckx P, Léonard S and van Eijk C W E 2006 Using Cramér–Rao theory combined with Monte Carlo simulations for the optimization of monolithic scintillator PET detectors *IEEE Trans. Nucl. Sci.* **53** 1063–70

Van Der Laan D J, Schaart D R, Maas M C, Beekman F J, Bruyndonckx R and van Eijk C W E 2010 Optical simulation of monolithic scintillator detectors using GATE/GEANT4 *Phys. Med. Biol.* **55** 1659–75

Van Elmpt W, McDermott L, Nijsten S, Wendling M, Lambin P and Mojnheer B 2008 A literature review of electronic portal imaging for radiotherapy dosimetry *Radiat. Oncol.* **88** 289–309

Visvikis D, Bardies M, Chiavassa S, Danford C, Kirov A, Lamare F, Maigne L, Staelens S and Taschereau R 2006a Use of the GATE Monte Carlo package for dosimetry applications *Nucl. Instrum. Methods Phys. Res.* A **569** 335–40

Visvikis D, Lefevre T, Lamare F, Kontaxakis G, Santos A and Darambaravan D 2006b Monte Carlo based performance assessment of different animal PET architectures using pixellated CZT detectors *Nucl. Instrum. Methods Phys. Res.* A **569** 225–9

Wang L, Jacques S L and Zheng L 1995 MCML—Monte Carlo modeling of light transport in multi-layered tissues *Comput. Methods Prog. Biomed.* **47** 131–46

Welsh J S, Bradley K, Ruchala K J, Mackie T R, Mañjon R, Patel R, Wiederholt P, Lock M, Hui S and Mehta M P 2004 Megavoltage computed tomography imaging: a potential tool to guide and improve the delivery of thoracic radiation therapy *Clin. Lung Cancer* **5** 303–6

Zahra N, Frisson T, Grevillot L, Lautesse P and Sarrut D 2010 Influence of Geant4 parameters on dose distribution and computation time for carbon ion therapy simulation *Phys. Medica* **26** 202–8